

Synthesis of PbTe/Pb quasi-one-dimensional nanostructure material arrays by electrodeposition

Zhaocun Zong,¹ Mingzhe Zhang,^{1,a)} Hongliang Lu,² Dan Xu,¹ Suangming Wang,¹ Huifang Tian,¹ Chang Liu,¹ Haiming Guo,² Hongjun Gao,² and Guangtian Zou¹

¹State Key Laboratory of Superhard Materials, Jilin University, Changchun 130012, People's Republic of China

²Institute of Physics, Chinese Academy of Sciences, Beijing 100190, People's Republic of China

(Received 23 January 2010; accepted 11 March 2010; published online 7 April 2010)

The ordered PbTe/Pb quasi-one-dimensional nanowires array was electrodeposited on the SiO₂/Si substrate. There are two essential factors for the formation of such kind of change in nanowire morphology and structure. One is the charges distribution at the tips of electrodeposit, the other one is the change in ion concentration in front of growth tip. We research the current versus bias voltage characteristics of single PbTe/Pb nanowire by four-probe scanning tunneling microscopy system. © 2010 American Institute of Physics. [doi:10.1063/1.3386262]

The synthesis and characterization of semiconductor nanostructures have been extensively investigated because of their importance in fundamental research and in the fabrication of nanoscale devices.¹ Especially, one-dimensional (1D) semiconductor nanostructures provide a good system to investigate the dependence of transport or mechanical properties on dimensionality and size reduction.² Although 1D nanostructures can be fabricated using a number of advanced techniques, the cost is usually quite high.³ Lead telluride is an important IV–VI semiconductor which is widely used in infrared detectors⁴ and thermoelectrics.⁵ Many functional structure materials based on lead telluride have been fabricated and displayed many new characters.⁶ There were various methods for synthesizing lead chalcogenide nanowires, including self-assembly,⁷ electrochemical deposition,⁸ and chemical vapor transport approach.⁵ Among these techniques, electrodeposition is unique because the driving force of reaction is precisely known and controllable.⁹

In this letter, we demonstrate the synthesis of PbTe/Pb quasi-one-dimensional nanostructure arrays by electrodeposition in ultrathin electrolyte layer on a SiO₂/Si substrate. We detailedly explain the formation mechanism of the unique morphology and structure in the process of electrodeposition. We also compare the resistance change in the single nanowire with different PbTe content and the influence of annealing process.

The PbTe/Pb quasi-one-dimensional parallel array is prepared on a SiO₂/Si substrate by an electrochemical cell, which consists of a piece of SiO₂/Si substrate and a clean cover glass plate. The setup for the electrodeposition is shown schematically in Fig. 1(a). The experimental details are given in Ref. 11.

The morphology of product was examined using field emission scanning electron microscopy (SEM, JSM-6700F) and the optical microscopy (Leica). The large area and ordered nanowire array was showed in Figs. 1(c) and 1(d). In the array, every nanowire was composed of periodic growth parts with changed diameter, and the length of nanowire could reach a few hundred microns. The length of every

growth period was about 3 μm. The structure characterization of product was given in Ref. 11.

In the electrodeposition process, the charges distribution at the tips of electrodeposit determined the morphology of nanomaterial.¹⁰ When the applied voltage is 0.4 V, the tip morphology corresponded to the wider part of nanowires, as seen in Figs. 2(a) and 2(b). After that, the applied voltage becomes 0.8 V, which would bring the changes of two main factors. On the one hand, the increase in potential would change the distribution of charges at the tips of nanowires. To the ordered nanowires array, the charges at every nanowire tip would suffer the excluded forces from the tip charges of contiguous nanowires. The suddenly increased charges would strengthen the mutual excluded forces, which would lead that the tip charges of all wires are further concentrated in the forefront of tips and the electric field lines become dense immediately. Thus, the nucleation region starts to shrink and the migrating cations would be mainly deoxidized on the forefront of growth tip. On the other hand, the increase in potential could quicken the deoxidized veloc-

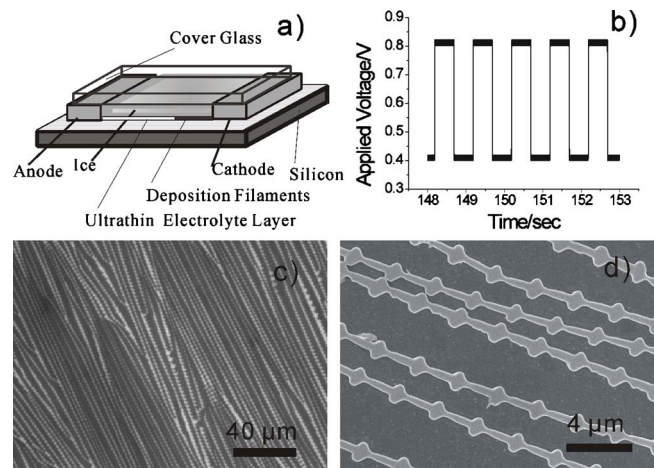


FIG. 1. (Color online) (a) Schematic showing the central configuration of electrochemical cell. (b) The applied voltage of electrodeposition which varies from 0.4 to 0.8 V in a square wave form with 1 Hz frequency. (c) Optical micrograph of PbTe/Pb nanostructure material arrays with a field of view of 200 μm (w) × 160 μm (h). (d) The representative SEM image of PbTe/Pb nanostructure arrays.

^{a)}Author to whom correspondence should be addressed. Electronic mail: zhangmz@jlu.edu.cn. Tel.: 086-0431-85166089.

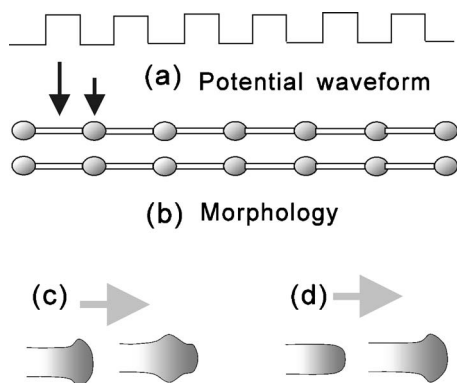


FIG. 2. [(a) and (b)] Schematic showing the correspondence relation between the applied voltage and the morphology of electrodeposits. The growth process in a period includes the two following parts: (c) the width of the electrodeposit change thin from wide and (d) the width of the electrodeposit change wide from thin.

ity of cations. As the variation in ion concentration near the growth front always lags behind the change in potential on the cathode.¹⁰ Although the potential have increased, the ion concentration near the tip of nanowires is still kept in the state correspond to the lower potential value. The moment concentration was deficient to the increased potential value and the cation near the tip of nanowires is almost exhausted immediately. In order to gain the plenitudinous cation, the depletion region of cation in front of tips begins to expand and the forward velocity of nanowires increase in electrolyte. The cation concentration is deficient in the growth process, which also could reduce the width of nanowires. The two main factors brought by the increased potential in the growth process not only reduce the width of nanowires, as seen in Fig. 2(c), but also quicken the growth velocity of nanowires.

When the potential becomes low again, the diameter of nanowires would change wide. The distribution of electric field lines and the change in ion concentration are exactly opposite to the states that the potential is high. The charges at the tips of nanowires would suffer weak excluded forces from the tips of contiguous nanowires, so the concentrated charges on the forefront of nanowires would disperse to the whole front of nanowires. The front electric field lines would become dispersive and the nucleation region of cations would expand gradually in the front of nanowires. Another factor is the change in ion concentration. When the potential changed low, a large number of cations that brought by the high potential still remain the transport state with the help of electromigration and ion diffusion. So the cations are superfluous to the low potential near the growth front and the nucleation region gradually starts to expand at the tips of nanowire. The rapid potential change from high to low would decelerate the deoxidized velocity of cations immediately and slow the growth velocity of nanowires. The two factors induce the nanowires to widen in the diameter, as seen in Fig. 2(d). The whole growth process had been recorded by using a CCD and could be observed clearly (Ref. 11).

Figure 3 shows the high-resolution transmission electron microscopy (HRTEM) images at different parts of the PbTe/Pb nanostructure. Figure 3(a) indicates nanoparticles are composed of element lead at the node part. Figure 3(b) shows that there are two kinds of crystal grains at the thin location of nanostructure material, Pb and PbTe. The HR-

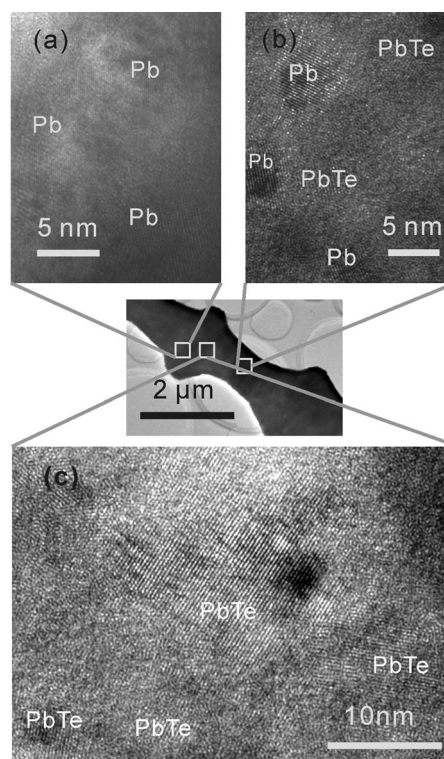


FIG. 3. HRTEM of electrodeposit at different locations. (a) HRTEM image at the wide part of electrodeposit shows lattice fringes spaced by 2.48 and 1.75 Å, corresponding to Pb (111) and (200) lattice-planes, respectively. (b) HRTEM image at the thin part of electrodeposit shows three groups of lattice fringes corresponding to the PbTe (200), PbTe (220), and Pb (111) lattice-planes. (c) HRTEM image at the transition zone from wide to thin part shows lattice fringes spaced by 3.2 and 2.87 Å corresponding to PbTe (200) and Pb (111) lattice-planes, respectively.

TEM image between the wide and the thin parts [Fig. 3(c)] shows that the PbTe layer is obvious but not complete in the area. As the different ions correspond to the different reduction potentials in the process of electrodeposition, the changes of potential and HTeO_2^+ concentration near the growth tip are the main factors fabricating the unique nanostructure. When the applied voltage is 0.4 V, both Pb^{2+} cations and HTeO_2^+ cations would be migrated to the front of the nanowires. As the reduction potential is lower, only Pb^{2+} could be deoxidized at the tip and the HTeO_2^+ cations would not be consumed. During the Pb^{2+} was deoxidized to metal Pb, the HTeO_2^+ concentration starts to increase in front of growth tip. After 0.5 s, the applied voltage becomes 0.8 V and the HTeO_2^+ cations could be deoxidized. As the HTeO_2^+ concentration is relatively high, the PbTe layer is first fabricated [as seen in Fig. 3(b)] and the accumulative HTeO_2^+ cations are consumed massively. With the reaction proceeding, HTeO_2^+ concentration gradually decrease and only partly PbTe grains are deoxidized. Thus, the PbTe grains and metal Pb are concomitant at the remaining part, as seen in Fig. 3(c).

In order to explore the effect of the structures and components of PbTe/Pb nanowires on their electronic transport properties, two kinds of PbTe/Pb nanowires were electrodeposited in the two different electrolytes with 0.001 M and 0.005 M HTeO_2^+ , respectively. The electrical measurements are performed by a ultrahigh vacuum four-probe scanning tunneling microscopy (4P-STM) system,¹² in which four independent tungsten (W) tips are used as the electrodes. Fig-

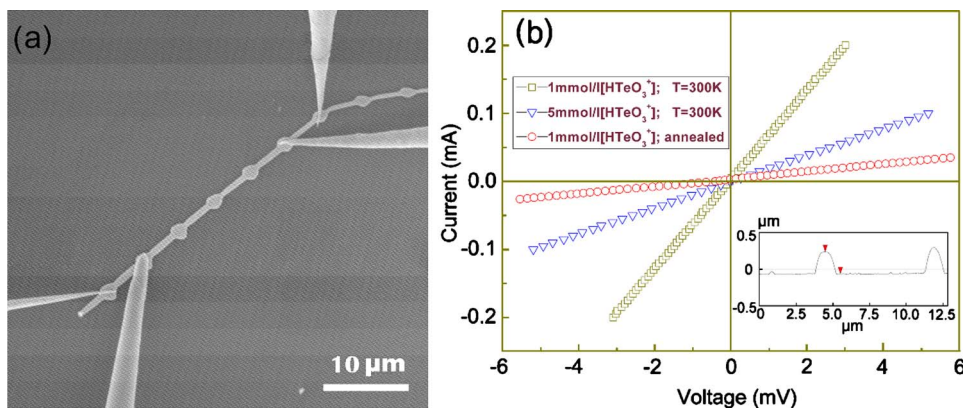


FIG. 4. (Color online) (a) SEM image of four-probe PbTe/Pb nanostructure material device. (b) The current-voltage characteristics of nanowires that corresponded to 0.001 and 0.005 M HTeO_2^+ concentrations and current-voltage characteristic of annealed nanowire. The inset gives the measured profiles of atomic force microscope at the thin parts of nanowires.

ure 4(a) shows a SEM image of four terminal electrical measurement on a single PbTe/Pb nanowire with four tips. The results of current versus bias voltage (I-V) characteristics of the PbTe/Pb nanostructures are given in Fig. 4(b). The measured profile of atomic force microscope shows the thickness of nanowire is about 300 nm. All of the I-V curves are linear under a high bias voltage. At 300 K, the resistivity of PbTe/Pb nanowires corresponding to 0.001 M HTeO_2^+ is calculated to be 318 nΩ m, which is slightly higher than the value of metal Pb. The result indicates the PbTe layer is incomplete and the charge transport of nanowires is mainly kept in metal region. The resistivity of PbTe/Pb nanowires corresponding to 0.005 M HTeO_2^+ is 1062 nΩ m, which means the conductance of nanowires decrease with the increase in PbTe content. In order to improve the crystallinity and reduce defect density, the single nanowire is annealed at 750 K for 30 min. It is demonstrated that after the annealing the resistivity of the nanowire corresponding to 0.001 M can increase about one order of magnitude, i.e., from 318 to 3816 nΩ m, which could be attributed to the higher crystallinity of PbTe grains in the annealed nanowire.

In conclusion, we have electrodeposited ordered PbTe/Pb quasi-one-dimensional nanowires array. The recurrent node structures and component gradient are attributed to the fluctuation of charge distribution and ion concentration at the growth ends of electrodeposit when the potential changes. The I-V characteristic of single PbTe/Pb nanowire shows the conductance of nanowires decrease with the increase in PbTe content. The annealing result implies the annealing could favor the construction of microstructure. The large-area and ordered arrays of the peculiar nanostructures may facilitate the fabrication of nanoscale devices.

This work was funded by the National Science Foundation of China, Grant Nos. 50672029, 90923032, and 20873052. It was also supported by the Ministry of Science and Technology of China, Grant No. 2005CB724404.

- ¹Y. Cui, Q. Q. Wei, H. K. Park, and C. M. Lieber, *Science* **293**, 1289 (2001); D. M. Whang, J. Song, Y. Mu, and C. M. Lieber, *Nano Lett.* **3**, 1255 (2003).
- ²Y. N. Xia, P. D. Yang, Y. G. Sun, Y. Y. Wu, B. Mayers, B. Gates, Y. D. Yin, F. L. Kim, and H. Q. Yan, *Adv. Mater. (Weinheim, Ger.)* **15**, 353 (2003).
- ³S. Matsui and Y. Ochiai, *Nanotechnology* **7**, 247 (1996); S. H. Hong, J. Zhu, and C. A. Mirkin, *Science* **286**, 523 (1999); J. A. Dagata, *ibid.* **270**, 1625 (1995).
- ⁴B. A. Akimov, A. V. Dmitriev, D. R. Khohlov, and L. I. Ryabova, *Phys. Status Solidi A* **137**, 9 (1993); A. Barros, E. Abramof, and P. Rappl, *J. Appl. Phys.* **99**, 024904 (2006).
- ⁵M. Fardy, A. I. Hochbaum, J. Goldberger, M. M. Zhang, and P. D. Yang, *Adv. Mater. (Weinheim, Ger.)* **19**, 3047 (2007); J. Heremans, C. Thrush, and D. Morelli, *J. Appl. Phys.* **98**, 063703 (2005).
- ⁶M. Dzero and J. Schmalian, *Phys. Rev. Lett.* **94**, 157003 (2005); E. Rodríguez, E. Jimenez, L. A. Padilha, A. A. R. Neves, G. J. Jacob, C. L. César, and L. C. Barbosa, *Appl. Phys. Lett.* **86**, 113117 (2005); T. C. Harman, P. J. Taylor, M. P. Walsh, and B. E. LaForge, *Science* **297**, 2229 (2002); H. Beyer, J. Nurnus, H. Bottner, A. Lambrecht, T. Roch, and G. Bauer, *Appl. Phys. Lett.* **80**, 1216 (2002).
- ⁷H. Tong, Y. J. Zhu, L. X. Yang, L. Li, and L. Zhang, *Angew. Chem. Int. Ed.* **45**, 7739 (2006); W. G. Lu, P. X. Gao, W. B. Jian, Z. L. Wang, and J. Y. Fang, *J. Am. Chem. Soc.* **126**, 14816 (2004).
- ⁸I. Enculescu, M. Sima, M. Enculescu, C. Ghica, M. Enache, and R. Neumann, *J. Optoelectron. Adv. Mater.* **9**, 1468 (2007); W. F. Liu, W. L. Cai, and L. Z. Yao, *Chem. Lett.* **36**, 1362 (2007); Y. Yang, S. C. Kung, D. K. Taggart, C. Xiang, F. Yang, M. A. Brown, A. G. Güell, T. J. Kruse, J. C. Hemminger, and R. M. Penner, *Nano Lett.* **8**, 2447 (2008).
- ⁹J. A. Switzer, C. J. Hung, B. E. Breyfogle, M. G. Shumsky, R. V. Leeuwen, and T. D. Golden, *Science* **264**, 1573 (1994).
- ¹⁰M. Z. Zhang, G. H. Zhuo, Z. C. Zong, H. Y. Cheng, Z. He, C. M. Yang, and G. T. Zuo, *Appl. Phys. Lett.* **88**, 203106 (2006); Z. C. Zong, H. Yu, L. P. Niu, M. Z. Zhang, C. Wang, W. Li, Y. F. Men, B. B. Yao, and G. T. Zuo, *Nanotechnology* **19**, 315302 (2008).
- ¹¹See supplementary material at <http://dx.doi.org/10.1063/1.3386262> for experimental details, the structure characterization, and the growth process video.
- ¹²X. Lin, X. B. He, T. Z. Yang, W. Guo, D. X. Shi, H. J. Gao, D. D. Ma, S. T. Lee, F. Liu, and X. C. Xie, *Appl. Phys. Lett.* **89**, 043103 (2006); X. J. Wang, J. F. Tian, T. Z. Yang, L. H. Bao, C. Hui, F. Liu, C. M. Shen, C. Z. Gu, N. S. Xu, and H. J. Gao, *Adv. Mater. (Weinheim, Ger.)* **19**, 4480 (2007).